

# On learning the right attention point for feature enhancement

Liqiang LIN<sup>1</sup>, Pengdi HUANG<sup>1</sup>, Chi-Wing FU<sup>2</sup>, Kai XU<sup>3</sup>,  
Hao ZHANG<sup>4</sup> & Hui HUANG<sup>1\*</sup>

<sup>1</sup>College of Computer Science and Software Engineering, Shenzhen University, Shenzhen 518060, China;

<sup>2</sup>Department of Computer Science and Engineering, The Chinese University of Hong Kong, Hong Kong 999077, China;

<sup>3</sup>School of Computer Science, National University of Defense Technology, Changsha 410073, China;

<sup>4</sup>School of Computing Science, Simon Fraser University, Burnaby V5A1S6, Canada

Received 7 October 2021/Revised 23 December 2021/Accepted 5 February 2022/Published online 23 December 2022

**Abstract** We present a novel attention-based mechanism to learn enhanced point features for point cloud processing tasks, e.g., classification and segmentation. Unlike prior studies, which were trained to optimize the weights of a pre-selected set of attention points, our approach learns to locate the best attention points to maximize the performance of a specific task, e.g., point cloud classification. Importantly, we advocate the use of single attention point to facilitate semantic understanding in point feature learning. Specifically, we formulate a new and simple convolution, which combines convolutional features from an input point and its corresponding learned attention point (LAP). Our attention mechanism can be easily incorporated into state-of-the-art point cloud classification and segmentation networks. Extensive experiments on common benchmarks, such as ModelNet40, ShapeNetPart, and S3DIS, all demonstrate that our LAP-enabled networks consistently outperform the respective original networks, as well as other competitive alternatives, which employ multiple attention points, either pre-selected or learned under our LAP framework.

**Keywords** point convolution, feature enhancement, attention point, deep neural network

**Citation** Lin L Q, Huang P D, Fu C-W, et al. On learning the right attention point for feature enhancement. Sci China Inf Sci, 2023, 66(1): 112107, <https://doi.org/10.1007/s11432-021-3431-9>

## 1 Introduction

Learning point features is one of the most fundamental problems in 3D vision and a key building block for tasks, such as shape classification and segmentation. Conventional convolution employs fixed kernels of varying sizes to aggregate point features, while extensions to variable neighborhoods, which account for anisotropy [1] and other local shape properties, have also been studied. Another line of approaches follows the non-local means idea [2] by collecting features at points that are similar to one another.

Recently, the use of selective attention [3–7] has gained much success in computer vision. In a typical setting, an attentional network computes the feature of a point by pre-selecting [8–10] a set of nearest points in the point's neighborhood and learning the associated attention weights to capture additional contextual information through the weights to enrich the point feature. Another recent approach resorts to finding non-local neighbors [11] by considering points within a much larger neighborhood.

In this paper, we present a new model for attentional point feature learning, which learns to locate a single attention point for feature enhancement to optimize the performance of a specific point cloud processing task, such as classification and segmentation. For example, to incorporate our model into a classification network, e.g., DGCNN [9], that is based on point-wise convolutional feature processing and aggregation, we can readily replace each convolution layer in the network (i.e., EdgeConv in the case of DGCNN) with a new convolution, which combines or fuses the convolutional feature at an input point with the convolutional feature at its corresponding learned attention point (LAP). Hence, while only one attention point is selected by our method, the feature fusion captures the information from two local

\* Corresponding author (email: [hhzhiyan@gmail.com](mailto:hhzhiyan@gmail.com))

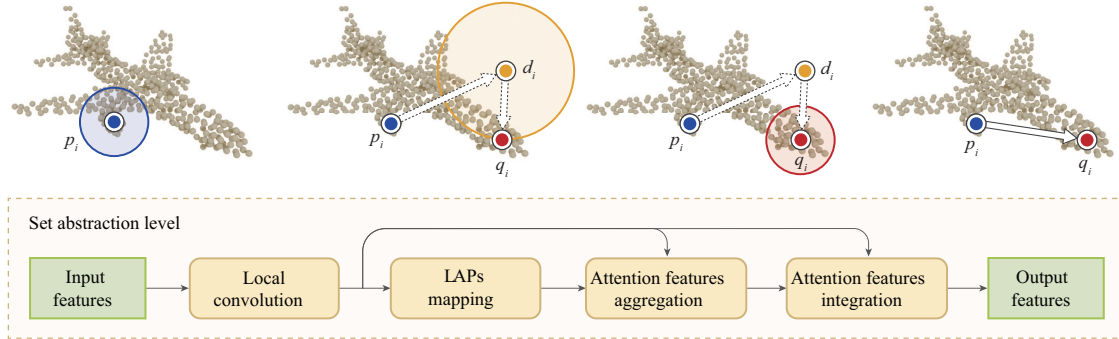


**Figure 1** (Color online) Learning to locate the best attention point  $q_i$  (red) for a given point  $p_i$  (blue). The feature  $f_i$  at  $p_i$  is updated using arbitrary local convolution. After that, we take  $f_i$  to learn an offset vector to obtain  $d_i$  (yellow), from which we locate the target attention point  $q_i$ . We then aggregate the neighboring features of  $q_i$ , which are finally fused into  $p_i$ 's features.

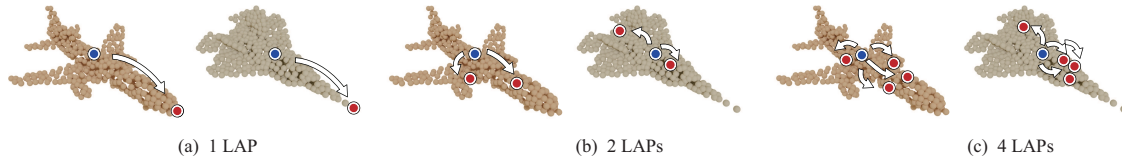


**Figure 2** (Color online) Visualizing different numbers of LAPs (red dots) selected by the same learning framework, for the same original points (blue dots) on two airplanes. More LAPs, two or four in (b) and (c), respectively, tend to exhibit less semantic consistency, compared with the single best LAP (a).

point neighborhoods. The LAP is obtained by adding to the original point an offset vector, as illustrated in Figure 1. These offset vectors are learned by minimizing the classification errors over the training point clouds.

Unlike prior attentional models, which were trained to optimize the weights of a pre-selected set of attention points [10, 11] or a sequence via a recurrent network [12], we focus on learning to locate one best LAP. A key premise of our work is that if the right point is found, then adding more attention may not be more effective. Our intuition is that as shape geometries and structures vary, e.g., within the same class of shapes for classification or within the same semantic part in the context of segmentation, it is easier to attain semantic consistency with one LAP than with more, as illustrated in Figure 2 for a comparison between one, two, and four LAPs. Such a consistency implies that matching points on two similar shapes (e.g., the two blue points on the two airplanes in each column of Figure 2) tend to be mapped to matching LAPs (the corresponding red points).

As shown in Figure 3, the attention points learned by our method do appear to exhibit a certain level of semantic understanding. Since our training is task-dependent, the LAPs tend to behave differently for different tasks. In particular, they may not possess similar features as the original points. The highlighted blue dots in Figure 3(a) are located in similar geometry: seat surface and desktop surface. For chairs, the LAPs (the highlighted red dots) are mapped to the chair backs, but there are no backs for desks. So the features of the blue dots can be complemented by the features of LAPs. This works similarly for a segmentation task. The highlighted blue dots in Figure 3(b) are located on the border between different semantic parts and thus share similar features. It is hard to discriminate them apart from a segmentation network. But with the different semantic features of the LAPs, they can be segmented in a more correct manner. A critical observation here is that for feature enhancement, points with dissimilar features can be equally useful since they can provide complementary information.

Our LAP-based attentional point feature learning mechanism can be easily incorporated into modern classification and segmentation networks, such as PointNet++ [13], RSCNN [14], DGCNN [9], and KP-Conv [15]. We show through comprehensive tests that, on common benchmarks ModelNet40, ShapeNet-Part, and S3DIS, our LAP-enabled networks consistently improve the performance over the respective original networks, as well as other competitive alternatives, which employ multiple attention points, either pre-selected, such as PointASNL [11] and PointWeb [10], or learned under our LAP framework. The consistent improvements are verified over varying point neighborhood sizes, train-test splits, and ways

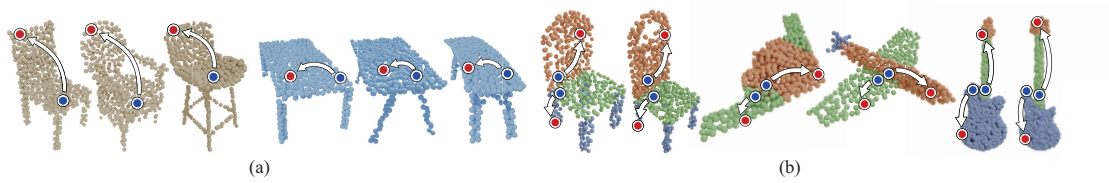


**Figure 3** (Color online) Learned attention points (LAPs) by our method, shown in red, corresponding to several original (blue) points on two tasks. For classification (a), the LAPs exhibit within-class semantic consistency, while helping to discriminate between different classes: attention points for similar original points on chair seats and tabletops are located on different semantic parts. For segmentation (b), the two blue points on each shape belong to different semantic regions, but are spatially close, thus sharing similar spatial neighborhoods. However, their LAPs are located far apart on different semantic parts, effectively “pushing” the blue points into different segments by making their features dissimilar.

for feature integration.

## 2 Related work

**Deep learning on 3D point clouds.** Inspired by the seminal work of PointNet [16], many deep neural networks have been developed to directly operate on points [17]. To overcome the inadequacy of PointNet on capturing local structures, PointNet++ [13] adopts a deep hierarchical feature learning mechanism that recursively employs PointNet to process point neighborhoods of increasing sizes. Later, PCNN [18] adapts image-based CNNs to the point cloud setting, leading to a permutation-invariant point feature learning. PointCNN [19] learns a transformation matrix to weight the input features associated with the input points and rearrange the points into a canonical permutation. A recent survey on this topic is available in [20].

One recent work of relevance is S-NET [21], a learning-based point cloud downsampling network that is also optimized for a particular task (e.g., classification or retrieval), like our work. Also, both their sampling problem and our proposed approach to feature enhancement would come down to learning to locate a small number of points that contribute most to a task at hand. While the success of their work can be seen as validation of our task-specific training, the problem setup and model design for attention point selection are completely different from S-NET.

**Point feature learning.** Point features play an important role in task performance. So, a majority of deep models on 3D point clouds focus on designing methods to extract better features, typically by exploiting a point’s local neighborhood. DGCNN [9] bases the neighboring relations of points on their distances in the feature space and aggregates pair-wise features to generate features for the center point. PointWeb [10] densely connects every pair of points in a local neighborhood, aiming at extracting point feature that better represents the local region around the center point. Ran et al. [22] explored the possibilities of local relation operators for point clouds.

Other methods focus on designing efficient convolution kernels [23,24] on points. PointConv [25] treats the convolution kernel as a Monte Carlo estimate of nonlinear functions of the local 3D coordinates of points. Point features are weighted by the estimated density. KPConv [15] uses a set of points in Euclidean space as the convolution kernel and aggregates input features based on the distances between kernel points and input points. PAConv [26] introduces a generic convolution operation for 3D point cloud processing. While prior studies focus mostly on learning local features, some recent ones [11,27] start to explore non-local 3D features with the attention mechanism [3].

**Attentional point feature learning.** Attention-based feature learning [3] has been introduced to learning point features soon after its applications to image features. Rather than being exhaustive, we discuss methods that focus on point feature learning rather than on specific vision tasks. Yang et al. [28] proposed the point attention transformer, which leverages a parameter-efficient group shuffle attention to learn the point relations. Zhang et al. [29] proposed point contextual attention network to predict the significance of each local point feature based on the point context. Chen et al. [30] learned local geometric representations by embedding a graph attention mechanism. Zhao et al. [31] designed self-attention layers and adapted a transformer for point clouds.

Further, attention can be used to learn long-range global features. Liu et al. [12] proposed Point2Sequence, an RNN-based model that captures correlations between different areas in a point cloud. Lu et al. [32] designed the spatial-channel attention module to capture multi-scale and global context

features. Han et al. [33] created a global graph and weights features of distant points with attention. More recently, Cheng et al. [27] proposed global-level blocks to update the feature of a superpoint using weighted features of other superpoints, while Yan et al. [11] proposed PointASNL that samples points over the whole point cloud to query similar ones for non-local point feature learning.

All the methods mentioned above pre-select a set of points, usually points in the local neighborhood or points with similar features, as the attentional points. In the 2D image domain, Zhang et al. [34] proposed to learn an affinity matrix for each attention point to shift it to a better location. The features of the attention points are weighted based on feature similarity. On the other hand, Xue et al. [35] suggested that not all attention is needed, and only a small part of the inputs is related to the output targets, through their investigations into several natural language processing tasks. Our work is inspired by these studies which employ learned attentional processing. Yet, we go beyond them and propose to learn to locate the point to attend to, over the entire point cloud, without relying on feature similarity.

### 3 Method

Recent deep learning approaches for 3D point clouds often focus on designing operators for better local feature extraction. Let  $f_i \in \mathbb{R}^{C_1}$  denote the input feature of point  $p_i$  in a certain network layer ( $C_1$  is the channel number). This local operator takes the input features of  $p_i$ 's neighbors and aggregates them to form the output feature  $f'_i \in \mathbb{R}^{C_2}$  of  $p_i$ ,

$$f'_i = \text{LocalConv}(\mathcal{N}(p_i)), \quad (1)$$

where  $\mathcal{N}(p_i)$  is the set of neighboring points of  $p_i$ , which are often found by a ball query or  $k$ -nearest neighbor (KNN) search. Here, LocalConv denotes a local convolution. It can be a point-wise local operator [13, 16], a grid kernel local operator [15], or an attention-based local operator [10].

Some methods use attention to learn global features for long-range structures, in which  $\mathcal{N}(p_i)$  is replaced by a set of pre-selected attention points. These points can be found by locating points with similar features as  $f_i$  in the feature space. Like (1), a basic mechanism is to weigh the input features of the attention points based on the feature similarity, then to combine them into the output feature of  $p_i$ .

In this study, we propose a new network module, called LAP-Conv, that directly learns to find attention points without relying on the feature similarity. In particular, we learn to find for each input point  $p_i$  only one attention point instead of finding multiple ones. The top part of Figure 1 illustrates how LAP-Conv works. Let  $P$  be the input cloud with  $n$  points  $\{p_1, p_2, \dots, p_n\}$ . Taking as an example the blue point in Figure 1 as  $p_i$ , we learn to find its associated attention point  $q_i$ , the red point, through the assistance of the offset point  $d_i$ , the yellow point.

The bottom part of Figure 1 shows the overall feature learning pipeline. First, we update feature  $f_i$  of point  $p_i$  using a local convolution block (Eq. (1)), and then map  $f_i$  to the corresponding attention point  $q_i$  using the LAPs mapping block (Subsection 3.1). Next, the attention features aggregation block (Subsection 3.2) aggregates features for the attention point  $q_i$ . Finally, the attention features integration block (Subsection 3.3) integrates the feature of the attention point into the output feature of  $p_i$ . Also, we show the detailed structure of LAP-Conv in Figure 4, in which the three blocks are outlined.

#### 3.1 Learning to locate attention points

The features of points in the point cloud are first updated with (1). We learn a function  $D$  to map the input feature of point  $p_i$  to locate offset point  $d_i$  (the yellow point in Figure 1) with  $d_i = D(f_i)$ , and then find the target attention point  $q_i$  (the red point) with the assistance of point  $d_i$ . Inspired by the way how neighboring points are found in the feature space [9], we propose to learn to find the attention points either in the Euclidean space or in the feature space.

Case (i). For attention points in the Euclidean space, we use a small MLP to map the feature  $f_i$  to a three-dimensional offset vector in the Euclidean space. We then add this vector back to the 3D coordinates  $x_i$  of the original point  $p_i$  to locate the offset point,

$$d_i = \text{MLP}(f_i) + x_i. \quad (2)$$

This MLP is shared among all the points in the input point cloud  $P$ . Also, point  $d_i$  is not necessarily a point in  $P$ . Its location is arbitrary in the Euclidean space. Hence, we map the feature of point  $p_i$

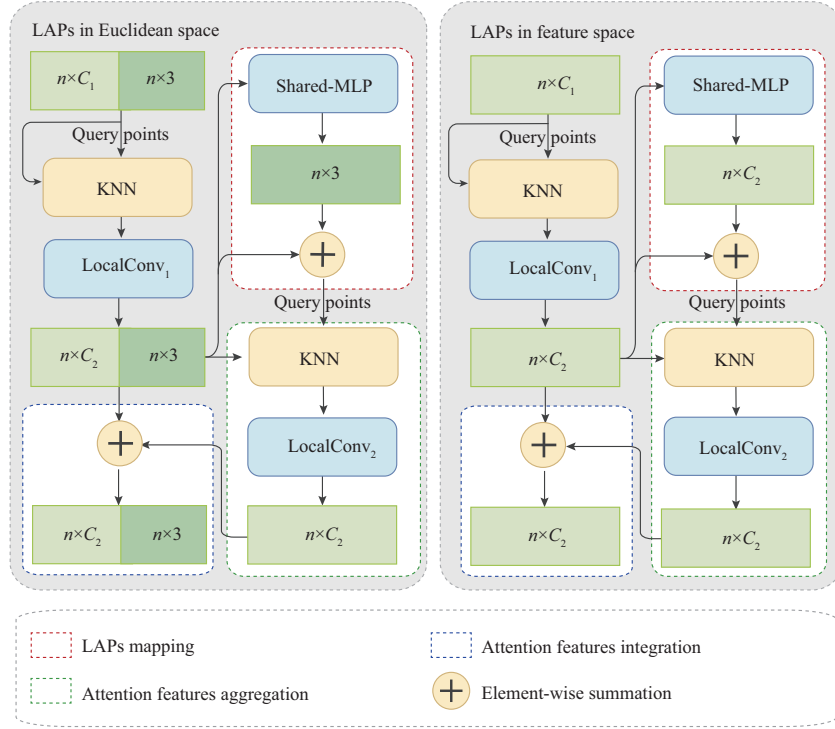


**Figure 4** (Color online) The structure of LAP-Conv. For each attention point in the Euclidean space, we learn a 3-dimensional offset vector and add it back. Each resulting point is used as a query point to find the  $k$ -nearest points in the point cloud. The features of these points are aggregated into the learned attention point and the feature of each attention point is integrated into the original feature. For attention points in the feature space, the offset vectors are in the same space and the neighboring points are also found in the feature space.

to an offset vector, which acts as an attention direction for further pinpointing  $d_i$ . Taking point  $d_i$  as guidance, we then find the nearest point  $q_i$  to point  $d_i$  among all the points in the entire point cloud as the learned attention point  $q_i$  associated with  $p_i$ .

Case (ii). For attention points in the feature space, the feature  $f_i$  of point  $p_i$  is mapped via a small shared MLP to an offset vector (with the same channel number as  $f_i$ ) in the feature space. This vector is then added to  $f_i$  to produce  $f_{d_i}$ , which is an offset feature in the feature space:

$$f_{d_i} = \text{MLP}(f_i) + f_i. \quad (3)$$

Similar to  $d_i$  in case (i), offset feature  $f_{d_i}$  is not necessarily a feature vector of the points in the original point cloud. Also, it can have arbitrary values. With  $f_{d_i}$ , we then search the entire point cloud for point  $q_i$  with the nearest feature vector  $f_{q_i}$  to  $f_{d_i}$  in the feature space, and take  $q_i$  as the corresponding learned attention point for point  $p_i$ . The blocks with the red-dotted frames in Figure 4 illustrate the detailed procedure of this LAPs mapping.

### 3.2 Attentional features aggregation

After finding the target attention point  $q_i$  for point  $p_i$ , we then aggregate the features of the neighborhood of  $q_i$  and update the feature of point  $q_i$  with

$$f_{q_i} = \text{LocalConv}(\mathcal{N}(q_i)). \quad (4)$$

For attention points in the Euclidean space, these neighboring points are found in the Euclidean space. For attention points in the feature space, these neighboring points are also found in the feature space.

To find the closest point  $q_i$  to  $d_i$ , we need to calculate the distances between point  $d_i$  and all the other points. To further find the neighboring points of  $q_i$ , another distance calculation is required.

To reduce the cost of processing two sets of distance calculations, we directly find the neighboring points of point  $d_i$  instead of explicitly finding point  $q_i$  and then its neighbors.

The learned attention point  $q_i$  must be among the neighboring points of  $d_i$ , since  $q_i$  is the nearest one to  $d_i$  in the original point cloud.

So, the feature of the learned attention point can be updated using the features of the neighboring points of  $d_i$  as

$$f_{q_i} = \text{LocalConv}(\mathcal{N}(d_i)). \quad (5)$$

For both cases (i) and (ii), we prefer to find these neighboring points using KNN. In this situation, no matter how large the offset vectors are, there are always neighboring points of  $d_i$ . If the neighboring points are found with a ball query [13], an additional loss is needed to punish the point  $d_i$  from being shifted too far away. Otherwise, there could be no neighboring points of  $d_i$  within a certain radius.

Hence, we use KNN to find the neighboring points for performing  $\text{LocalConv}_1$  for consistency. After we learn the offset points, we use them as query points to find  $k$  neighboring points and update the feature of  $q_i$ , as shown in the green dotted frames in Figure 4.

It should be noticed that all these neighboring points are points from the original point cloud (case (i)) or the features of the points in the original point cloud (case (ii)), in which  $d_i$  or  $f_{d_i}$  is not one of them.

### 3.3 Integration of attentional features

After we aggregate a feature for the learned attention point  $q_i$ , we then integrate the feature into the feature of  $p_i$  with an integration function  $I$  (' $I$ ' for integration):

$$f'_i = I(\text{LocalConv}_1(\mathcal{N}(p_i)), \text{LocalConv}_2(\mathcal{N}(d_i))), \quad (6)$$

where we could use the same or different convolutional operators for  $\text{LocalConv}_1$  and  $\text{LocalConv}_2$ .

In the previous attention-based networks for processing point clouds, e.g., [9–11, 27, 28, 33, 36, 37], the features of the attention points are weighted by a dot-product similarity between the features of the pre-selected attention points and  $p_i$ , or by the similarity in the spatial location between them. An attention point with a more similar feature is given a larger weight when added into the feature of  $p_i$ . However, we argue that not only points with similar features could be useful, but also points with different features could also be useful in feature learning. Particularly, points with different features could supply the center point  $p_i$  with vital context for performing the target task.

Here, one straightforward choice for  $I$  is to simply add the features of points  $q_i$  and  $p_i$  together:

$$I = \text{Add}(f_{p_i}, f_{q_i}), \quad (7)$$

as illustrated in the blue dotted frames in Figure 4. Since  $\text{LocalConv}_1$  and  $\text{LocalConv}_2$  do not share parameters, the network can learn to update the feature of  $q_i$  for adding it into the feature of  $p_i$ . Another choice for  $I$  is to concatenate the two features, and then use an MLP to reduce the dimensions:

$$I = \text{MLP}(\text{Concatenate}(f_{p_i}, f_{q_i})). \quad (8)$$

A comparison result between these two forms of feature integration can be found in Section 4.

## 4 Results and evaluation

Our proposed LAP-Conv can be easily adapted into conventional point-wise feature learning networks.

In existing networks, a  $\text{LocalConv}$  block is generally used in a set abstraction level to update the input feature  $f_i$  of a point and produce  $f'_i$ , as described in (1).

Hence, by keeping the channel sizes of the input and output features to be the same, we can replace the  $\text{LocalConv}$  block in existing networks with our LAP-Conv to boost the network performance.

To demonstrate the effectiveness of our LAP-Conv, we adapt it into common networks, including PointNet++ [13], RSCNN [14], DGCNN [9], and KPConv [15], producing LAP-enabled networks, i.e., LAP-PointNet++, LAP-RSCNN, LAP-DGCNN, and LAP-KPConv.

Note that since DGCNN finds neighboring points in feature space, the attention points for LAP-DGCNN are learned in the feature space (Eq. (2)). For the other LAP-enabled networks, the LAPs are learned in Euclidean space (Eq. (3)).

We conduct experiments using these networks on various tasks, including shape classification (Subsection 4.1), part segmentation, and semantic segmentation (Subsection 4.2), showing both quantitative comparisons and qualitative results. At last, we evaluate various aspects of our LAP-Conv (Subsection 4.3), e.g., one vs. multiple learned attention points, neighborhood sizes, train/test split, etc.

**Table 1** 3D shape classification results on ModelNet40<sup>a)</sup>

Method	Input	#points	OA
PointNet [13]	xyz	1k	89.2
PAT [28]	xyz+nor	1k	91.7
PointCNN [19]	xyz	1k	92.2
PointWeb [10]	xyz+nor	1k	92.3
PointConv [25]	xyz+nor	1k	92.5
A-CNN [24]	xyz	1k	92.6
Point2Node [33]	xyz	1k	93.0
PointASNL [11]	xyz	1k	92.9
PointASNL [11]	xyz+nor	1k	93.2
DensePoint [40]	xyz	1k	93.2
PointTransformer [31]	xyz	1k	93.7
GDANet [22]	xyz	1k	93.8
PACConv [26]	xyz	1k	93.9
PointNet++ [13]	xyz	1k	90.7
RSCNN [14]	xyz	1k	91.7
KPConv [15]	xyz	7k	91.9
DGCNN [9]	xyz	1k	92.9
SimpleView-PointNet++ [41]	xyz	1k	91.2
SimpleView-RSCNN [41]	xyz	1k	93.3
SimpleView-DGCNN [41]	xyz	1k	93.9
LAP-PointNet++	xyz	1k	92.9
LAP-RSCNN	xyz	1k	92.8
LAP-KPConv	xyz	7k	92.3
LAP-DGCNN	xyz	1k	<b>93.9</b>

a) OA: overall accuracy (%); xyz: points only as input; xyz+nor: use points and normals.

## 4.1 Classification

First, we evaluate our method on the shape classification task using ModelNet40 [38], which provides a comprehensive collection of 12311 CAD models from 40 categories. Here, we use the input point clouds sampled from these models by PointNet [16]. Typically, 1024 points are uniformly sampled per model to serve as the network input.

Following the official train/test split, we use 9843 models for training and 2468 models for testing.

In this experiment, we evaluate the performance of LAP-PointNet++, LAP-RSCNN, LAP-KPConv, and LAP-DGCNN, where data preprocessing, augmentation, and the choice of hyper-parameters all follow the original network settings. Also, we employ only 3D point coordinates as network inputs.

For LAP-PointNet++, the training epochs are 500, the batch size is 24, and the learning rate is 0.001. For LAP-RSCNN, since only the single-scale version of the RSCNN code is officially released, we develop our LAP-RSCNN based on the released code and report 91.7 for the single-scale RSCNN, following [39]. The training epochs are 120, the batch size is 32, and the learning rate is 0.001.

In this paper, we report 91.9 for KPConv as the result reproduced by the officially released code. The training epochs are 400, the batch size is 16, and the learning rate is 0.001 for LAP-KPConv.

For LAP-DGCNN, the training epochs are 500, the batch size is 32, and the learning rate is 0.001.

Table 1 [40, 41] reports the results of using different methods for the shape classification task. Comparing the results of the three LAP-enabled networks with those of the original counterparts, we can see that all of them improve the performance over the original networks, showing that our LAP-Conv can help improve the quality of the features for the shape classification task.

Overall, LAP-DGCNN attains a higher performance with an overall accuracy of 93.9 on the classification task compared with other attention-based methods such as PointWeb [10], Point2Node [33], PointASNL [11], and PointTransformer [31].

## 4.2 Segmentation

**Part segmentation.** The ShapeNet Part dataset [42] has 16881 shapes over 16 categories and with 50 part labels. We sample 2048 points per shape from this dataset for our experiments and follow the official

**Table 2** Part segmentation results on ShapeNet Part dataset

Method	mIoU
Kd-Net [44]	82.3
PointNet [16]	83.7
PCNN [18]	85.1
PointTransformer [31]	86.6
PointNet++ [13]	85.1
DGCNN [9]	85.2
RSCNN [14]	86.2
KPConv [15]	86.4
LAP-PointNet++	85.4
LAP-DGCNN	85.8
LAP-RSCNN	86.4
LAP-KPConv	<b>86.9</b>

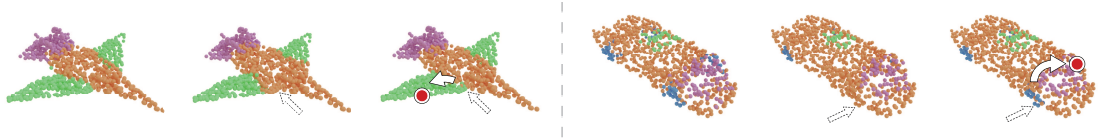


**Figure 5** (Color online) Comparing part segmentation on ShapeNet Part between PointNet++ and LAP-PointNet++. In each case, we present the input point cloud with ground-truth segmentation labels (left), segmentation results predicted by PointNet++ (middle), and segmentation results predicted by LAP-PointNet++ (right), respectively. We highlight an incorrectly labeled point near a segmentation boundary (hollow arrow) by PointNet++ (middle) and show the use of LAP-Conv (right) to correct the label with feature enhancement by an attention point (large red dot).

data split setup [43] adopted in DGCNN [9] and PointNet++ [13]. The batch size for LAP-PointNet++ is 16, the training epochs for LAP-RSCNN are 200, and the learning rate for LAP-KPConv is 0.01. Other parameters stay the same as on ModelNet40.

Table 2 [44] reports the performance by various methods, in terms of the mean intersection-over-union (mIoU) metric, showing that LAP-Conv helps improve the part segmentation performance of PointNet++, RSCNN, DGCNN, and KPConv. Figure 5 visually contrasts PointNet++ and LAP-PointNet++ to show the differences made by LAP-Conv.

**Indoor scene semantic segmentation.** We use the Stanford 3D large-scale indoor spaces (S3DIS) dataset [45], which contains large-scale 3D-scanned point clouds for six indoor areas with 272 rooms from three different buildings. Altogether, the dataset has  $\sim 273$  million points, each belonging to one of 13 semantic categories. Area-5 is used as the test scene for evaluating the method’s generalizability.

For LAP-DGCNN, each room is split into blocks of size  $1\text{ m} \times 1\text{ m}$  as done in DGCNN. The input is point coordinates together with RGB colors and normalized spatial coordinates (a 9D vector per point), following the settings in DGCNN [9]. During the training, we sample 4096 points from each room block. Then, all sampled points are used for testing. The training epochs are 500, the batch size is 10, and the learning rate is 0.01.

For LAP-KPConv, each 3D scene in the dataset is segmented into small sub-clouds contained in spheres. During the training, the spheres were picked randomly in the scenes, and during testing, they are picked regularly in the point clouds. The training epochs are 100, the batch size is 32, and the learning rate is 0.01.

Table 3 [46–51] gives the results, showing that LAP-Conv helps improve semantic segmentation performance on S3DIS for both DGCNN and KPConv.

Also, we present two visual semantic segmentation results on S3DIS in Figure 6.

Note that since PointNet++ and RSCNN did not report their results on S3DIS, LAP-PointNet++ and LAP-RSCNN are not evaluated on S3DIS.

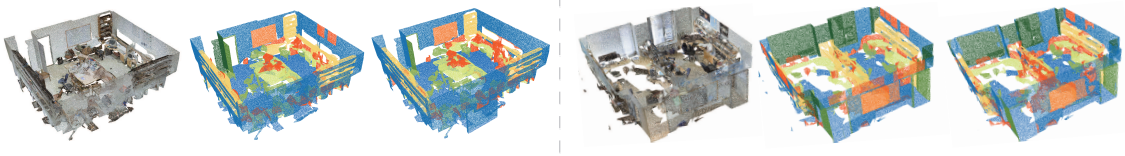
### 4.3 Ablation study

Finally, we evaluate various aspects of our method, employing LAP-DGCNN to test on ModelNet40.



**Table 3** Semantic segmentation results on the S3DIS dataset (evaluated on Area-5)

Method	mAcc	mIoU
PointNet [16]	49.0	41.1
TangentConv [46]	62.2	52.6
PointCNN [19]	63.9	57.3
SPGraph [47]	66.5	58.0
PointWeb [10]	66.6	60.3
HPEIN [48]	68.3	61.9
Point2Node [33]	70.0	63.0
MinkowskiNet [49]	71.7	65.4
BAAF-Net [50]	–	65.4
PACConv [26]	73.0	66.6
JSENet [51]	–	67.7
PointTransformer [31]	76.5	<b>70.4</b>
DGCNN [9]	59.1	53.1
KPConv [15]	72.8	67.1
LAP-DGCNN	62.3	53.6
LAP-KPConv	73.4	68.2

**Figure 6** (Color online) Visualization of two semantic segmentation results on S3DIS. In each case, we present the input point cloud with RGB colors (left), points with ground-truth semantic labels (middle), and segmentation results predicted by LAP-DGCNN (right), respectively.

**Different ways of choosing LAPs.** In this experiment, we compare LAP-DGCNN with three variants of the network in terms of how to choose attention points.

- Random-LAP-DGCNN, in which we replace the MLP for learning to generate the offsets (Eq. (3)) with a randomly-generated vector, thus replacing the core of our LAP-Conv, which uses the learned offset vector to locate the learned attention point.
- LAP2-DGCNN and LAP4-DGCNN, which respectively learns two and four attention points simultaneously, instead of one, in one single LAP-Conv module.

As comparison results in Table 4 shown, Random-LAP-DGCNN hardly makes any improvement over the baseline, which is DGCNN. The use of random attention points makes the network converge much slower than that of the baseline DGCNN. However, after adequate training epochs, the weights for those random attention points turn out to be very small numbers (most of them are zeros). Under this circumstance, LAP-DGCNN with random attention points degenerates into the DGCNN and thus leads to similar results.

This result demonstrates the importance of the learned offset vectors for searching for the target attention point.

Yet, using just the right learned attention point, as in LAP-DGCNN, we can achieve a large performance improvement over the original DGCNN.

Next, comparing LAP2-DGCNN and LAP4-DGCNN with LAP-DGCNN, we can see that learning to find and use more than one attention point improves over DGCNN. However, the improvement is far below that of using just one single learned attention point. Yet, an interesting observation is that the more learned attention points we use, resulting in larger network capacity, the worse the results appear to be, indicating that LAP's effectiveness is not merely brought by more convolution layers.

The visualization in Figure 2 on where the 1, 2, and 4 attention points were selected by the networks may hint at a possible reason: as more points are added, their consistency tends to drop.

As shown in Table 4, LAP4-DGCNN has 4.49 M parameters and DGCNN has 4.21 M parameters. Memory consumption has the same ratio as the amount of parameters. The runtime is 1.8 vs. 2.1 ( $10^{-2}$ /batch).

**Table 4** Comparing different ways of choosing LAPs

	OA	mAcc	Parameter (M)
DGCNN (baseline)	92.9	90.2	4.21
Random-LAP-DGCNN	93.0	89.9	4.25
LAP-DGCNN	<b>93.9</b>	<b>91.5</b>	4.28
LAP2-DGCNN	93.3	90.2	4.35
LAP4-DGCNN	93.1	90.3	4.49

**Table 5** Comparing different ways of integrating features

Different function $I$	OA	mAcc
$I_1$ or Eq. (7)	93.9	91.5
$I_2$ or Eq. (8)	93.6	91.0

**Table 6** Comparing different neighboring sizes ( $k$ ) in KNN

$k$	DGCNN	LAP-DGCNN
5	90.5	<b>93.5</b>
10	91.4	<b>93.4</b>
20	92.9	<b>93.9</b>
40	92.4	<b>93.3</b>

**Table 7** Shape classification results (OA) on ModelNet40 with different train/test splits

Train/all	DGCNN	LAP-DGCNN
80%	92.9	<b>93.9</b>
60%	91.5	<b>92.6</b>
40%	90.6	<b>92.1</b>
20%	88.9	<b>90.2</b>
10%	87.3	<b>88.0</b>
5%	82.7	<b>83.1</b>
1%	63.5	<b>64.9</b>

**Different feature integration.** We can have different ways of integrating the feature of point  $p_i$  with that of its LAP  $q_i$ ; see Subsection 3.3.

As shown in Table 5, option  $I_1$  (Eq. (7)) gives a slightly better performance compared with  $I_2$  (Eq. (8)), so we empirically choose  $I$  in our LAP-Conv. We have tested other ways of feature integration, e.g., point-wise multiply, but they do not lead to good results.

**Different neighborhood sizes.** Note that we built LAP-DGCNN by following the setting of DGCNN to use  $k=20$  for the two KNN operations in LAP-Conv. In this experiment, we test LAP-DGCNN with different neighboring sizes ( $k$ ), while keeping all the other settings unchanged.

As shown by the results in Table 6, the performance of our LAP-DGCNN is quite robust against different choices of  $k$ , and it also consistently outperforms DGCNN. Even with a rather small neighborhood size  $k=5$ , our method can already attain a rather high performance, which exceeds that of DGCNN for all the neighborhood sizes shown in Table 6.

**Different train/test splits.** In a final experiment, we test the robustness of our method over different training/test splits. Note that the original setting uses 9843 models, which is around 80% of the whole dataset for training, and the remaining 20% for testing.

We test the performance of our LAP-DGCNN using smaller training sets, from 80% down to 1% of the whole dataset, and compare with DGCNN, with results shown in Table 7. Similar to [52], we select the training samples as follows: for all train/test splits, we randomly sample one object per class first; the remaining training data are randomly sampled from the original training set, regardless of their classes. As we can observe from Table 7, our method performs well even with a very small training set, and most importantly, it consistently outperforms DGCNN over all train/test splits. Also, the randomization during our setup of the multiple training sets can alleviate potential concerns of over-fitting.

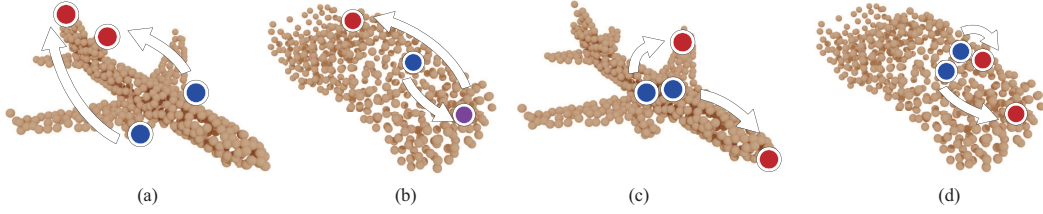


**Figure 7** (Color online) LAP selection learned by our network is neither symmetric (a) nor invertible (b), in general; and it is not always stable, as shown in (c) and (d), because nearby points may be mapped afar.

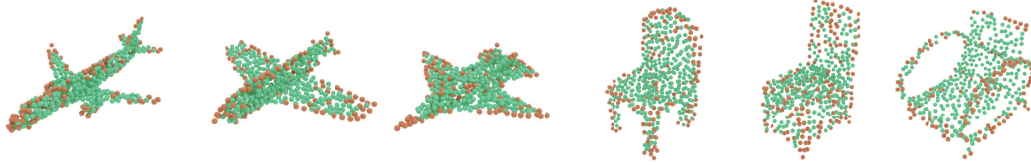


**Figure 8** (Color online) The LAPs are highlighted in orange while the original point clouds are in green.

## 5 Discussion, limitation, and future work

Our paper is about learning point features, which is an essential step in most point cloud processing tasks including classification, segmentation, and more. Furthermore, we tackle arguably the most fundamental question in this setting, namely, how to find the neighbors of a point  $P$  to best characterize its features. With deep learning, many studies proposed to learn what  $P$ 's neighbors are and their weights, as discussed in Section 2. Our work improves upon these attentional learning methods and it is motivated by two key observations: (a) the learning of attention points should be task-specific; and (b) one attention point may be best as it is easier to attain semantic consistency; see Figure 2. The merit of our ideas has been validated through a comprehensive evaluation, demonstrating that our one-LAP approach outperforms the use of multiple attention points, both by previous studies (e.g., PointASNL [11], PointWeb [10]), and when they are learned under our framework.

Currently, our LAP selection is neither symmetric nor invertible in general. As shown in Figure 7, if two points  $p$  and  $q$  are symmetric on a shape,  $LAP(p)$  and  $LAP(q)$  may not be, and  $p \neq LAP(LAP(p))$ . Figure 7 also shows that the selection may become unstable, as one would expect from the results of a data-driven optimization. However, it is worth noting that in general, we find that the learned offset vectors are more stable than the final attention points, which are obtained by projecting back onto the point clouds. Figure 8 shows the LAPs for each shape. The LAPs are usually mapped to some distinctive and characteristic regions, such as points on the edges or at tips.

On the technical front, our method may not extend to other representations such as voxels. In voxel-based representation, the offset points need to be discretized into voxels which may cause discontinuity in gradients.

**Acknowledgements** This work was supported in part by National Natural Science Foundation of China (Grant Nos. U21B2023, 62161146005, U2001206, 61902254), Guangdong Talent Program (Grant No. 2019JC05X328), Guangdong Science and Technology Program (Grant No. 2020A0505100064), DEGP Key Project (Grant Nos. 2018KZDXM058, 2020SFKC059), Shenzhen Science and Technology Innovation Program (Grant Nos. JCYJ20210324120213036, RCJC20200714114435012), HKSAR (Grant No. CUHK14206320), NSERC (Grant No. 611370), and Guangdong Laboratory of Artificial Intelligence and Digital Economy (SZ). We thank all anonymous reviewers for their valuable comments.

**Supporting information** Appendixes A and B. The supporting information is available online at [info.scichina.com](http://info.scichina.com) and [link.springer.com](http://link.springer.com). The supporting materials are published as submitted, without typesetting or editing. The responsibility for scientific accuracy and content remains entirely with the authors.

## References

- 1 Weickert J. Anisotropic diffusion in image processing. B.G. Teubner Stuttgart, 1998

- 2 Buades A, Coll B, Morel J M. A non-local algorithm for image denoising. In: Proceedings of IEEE Conference on Computer Vision & Pattern Recognition, 2005. 60–65
- 3 Vaswani A, Shazeer N, Parmar N, et al. Attention is all you need. In: Proceedings of Conference on Neural Information Processing Systems, 2017. 5998–6008
- 4 Liu X, Xia T, Wang J, et al. Fully convolutional attention networks for fine-grained recognition. 2016. ArXiv:1603.06765
- 5 Wang F, Jiang M, Qian C, et al. Residual attention network for image classification. In: Proceedings of IEEE Conference on Computer Vision & Pattern Recognition, 2017. 3156–3164
- 6 Peng Y X, He X T, Zhao J J. Object-part attention model for fine-grained image classification. *IEEE Trans Image Process*, 2018, 27: 1487–1500
- 7 Mnih V, Heess N, Graves A, et al. Recurrent models of visual attention. In: Proceedings of Conference on Neural Information Processing Systems, 2014. 2204–2212
- 8 Hamilton W, Ying Z, Leskovec J. Inductive representation learning on large graphs. In: Proceedings of Conference on Neural Information Processing Systems, 2017. 1024–1034
- 9 Wang Y, Sun Y, Liu Z, et al. Dynamic graph CNN for learning on point clouds. *ACM Trans Graph*, 2019, 38: 146
- 10 Zhao H, Jiang L, Fu C W, et al. PointWeb: enhancing local neighborhood features for point cloud processing. In: Proceedings of IEEE Conference on Computer Vision & Pattern Recognition, 2019. 5565–5573
- 11 Yan X, Zheng C, Li Z, et al. PointASNL: robust point clouds processing using nonlocal neural networks with adaptive sampling. In: Proceedings of IEEE Conference on Computer Vision & Pattern Recognition, 2020. 5589–5598
- 12 Liu X, Han Z, Liu Y S, et al. Point2Sequence: learning the shape representation of 3D point clouds with an attention-based sequence to sequence network. In: Proceedings of AAAI Conference on Artificial Intelligence, 2019. 8778–8785
- 13 Qi C R, Yi L, Su H, et al. PointNet++: deep hierarchical feature learning on point sets in a metric space. In: Proceedings of Conference on Neural Information Processing Systems, 2017. 5099–5108
- 14 Liu Y, Fan B, Xiang S, et al. Relation-shape convolutional neural network for point cloud analysis. In: Proceedings of IEEE Conference on Computer Vision & Pattern Recognition, 2019. 8895–8904
- 15 Thomas H, Qi C R, Deschard J E, et al. KPConv: flexible and deformable convolution for point clouds. In: Proceedings of International Conference on Computer Vision, 2019. 6411–6420
- 16 Qi C R, Su H, Mo K, et al. PointNet: deep learning on point sets for 3D classification and segmentation. In: Proceedings of IEEE Conference on Computer Vision & Pattern Recognition, 2017. 652–660
- 17 Riegler G, Ulusoy A O, Geiger A. OctNet: learning deep 3D representations at high resolutions. In: Proceedings of IEEE Conference on Computer Vision & Pattern Recognition, 2017. 3577–3586
- 18 Atzmon M, Maron H, Lipman Y. Point convolutional neural networks by extension operators. *ACM Trans Graph*, 2018, 37: 1–12
- 19 Li Y, Bu R, Sun M, et al. PointCNN: convolution on  $\chi$ -transformed points. In: Proceedings of Conference on Neural Information Processing Systems, 2018. 820–830
- 20 Guo Y, Wang H, Hu Q, et al. Deep learning for 3D point clouds: a survey. *IEEE Trans Pattern Anal Mach Intell*, 2021, 43: 4338–4364
- 21 Dovrat O, Lang I, Avidan S. Learning to sample. In: Proceedings of IEEE Conference on Computer Vision & Pattern Recognition, 2019
- 22 Xu M, Zhang J, Zhou Z, et al. Learning geometry-disentangled representation for complementary understanding of 3D object point cloud. In: Proceedings of the AAAI Conference on Artificial Intelligence, 2021. 3056–3064
- 23 Boulch A. ConvPoint: continuous convolutions for point cloud processing. *Comput Graphics*, 2020, 88: 24–34
- 24 Komarichev A, Zhong Z, Hua J. A-CNN: annularly convolutional neural networks on point clouds. In: Proceedings of IEEE Conference on Computer Vision & Pattern Recognition, 2019. 7421–7430
- 25 Wu W, Qi Z, Fuxin L. PointConv: deep convolutional networks on 3D point clouds. In: Proceedings of IEEE Conference on Computer Vision & Pattern Recognition, 2019. 9621–9630
- 26 Xu M, Ding R, Zhao H, et al. PConv: position adaptive convolution with dynamic kernel assembling on point clouds. In: Proceedings of the IEEE/CVF Conference on Computer Vision and Pattern Recognition, 2021. 3173–3182
- 27 Cheng M, Hui L, Xie J, et al. Cascaded non-local neural network for point cloud semantic segmentation. 2020. ArXiv:2007.15488
- 28 Yang J, Zhang Q, Ni B, et al. Modeling point clouds with self-attention and Gumbel subset sampling. In: Proceedings of IEEE Conference on Computer Vision & Pattern Recognition, 2019. 3323–3332
- 29 Zhang W, Xiao C. PCAN: 3D attention map learning using contextual information for point cloud based retrieval. In: Proceedings of IEEE Conference on Computer Vision & Pattern Recognition, 2019. 12436–12445
- 30 Chen C, Fragonara L Z, Tsourdos A. GAPNet: graph attention based point neural network for exploiting local feature of point cloud. 2019. ArXiv:1905.08705
- 31 Zhao H, Jiang L, Jia J, et al. Point transformer. In: Proceedings of the IEEE/CVF International Conference on Computer Vision, 2021. 16259–16268
- 32 Lu H, Chen X, Zhang G, et al. SCANet: spatial-channel attention network for 3D object detection. In: Proceedings of International Conference on Acoustics, Speech & Signal Processing, 2019. 1992–1996
- 33 Han W, Wen C, Wang C, et al. Point2Node: correlation learning of dynamic-node for point cloud feature modeling. In: Proceedings of AAAI Conference on Artificial Intelligence, 2020. 10925–10932
- 34 Zhang L, Xu D, Arnab A, et al. Dynamic graph message passing networks. In: Proceedings of IEEE Conference on Computer Vision & Pattern Recognition, 2020. 3726–3735
- 35 Xue L, Li X, Zhang N L. Not all attention is needed: gated attention network for sequence data. In: Proceedings of AAAI Conference on Artificial Intelligence, 2020. 6550–6557
- 36 Xie S, Liu S, Chen Z, et al. Attentional ShapeContextNet for point cloud recognition. In: Proceedings of IEEE Conference on Computer Vision & Pattern Recognition, 2018. 4606–4615
- 37 Liang Z, Yang M, Wang C. 3D graph embedding learning with a structure-aware loss function for point cloud semantic instance segmentation. 2019. ArXiv:1902.05247
- 38 Wu Z, Song S, Khosla A, et al. 3D ShapeNets: a deep representation for volumetric shapes. In: Proceedings of IEEE Conference on Computer Vision & Pattern Recognition, 2015. 1912–1920
- 39 Li R, Li X, Heng P A, et al. PointAugment: an auto-augmentation framework for point cloud classification. In: Proceedings of IEEE Conference on Computer Vision & Pattern Recognition, 2020. 6378–6387
- 40 Liu Y, Fan B, Meng G, et al. DensePoint: learning densely contextual representation for efficient point cloud processing.

- In: Proceedings of International Conference on Computer Vision, 2019. 5239–5248
- 41 Goyal A, Law H, Liu B, et al. Revisiting point cloud shape classification with a simple and effective baseline. In: Proceedings of International Conference on Machine Learning, 2021
- 42 Yi L, Kim V G, Ceylan D, et al. A scalable active framework for region annotation in 3D shape collections. *ACM Trans Graph*, 2016, 35: 1–12
- 43 Chang A X, Funkhouser T, Guibas L, et al. ShapeNet: an information-rich 3D model repository. 2015. ArXiv:1512.03012
- 44 Klovov R, Lempitsky V. Escape from cells: deep Kd-networks for the recognition of 3D point cloud models. In: Proceedings of International Conference on Computer Vision, 2017. 863–872
- 45 Armeni I, Sener O, Zamir A R, et al. 3D semantic parsing of large-scale indoor spaces. In: Proceedings of IEEE Conference on Computer Vision & Pattern Recognition, 2016. 1534–1543
- 46 Tatarchenko M, Park J, Koltun V, et al. Tangent convolutions for dense prediction in 3D. In: Proceedings of IEEE Conference on Computer Vision & Pattern Recognition, 2018. 3887–3896
- 47 Landrieu L, Simonovsky M. Large-scale point cloud semantic segmentation with superpoint graphs. In: Proceedings of IEEE Conference on Computer Vision & Pattern Recognition, 2018. 4558–4567
- 48 Jiang L, Zhao H, Liu S, et al. Hierarchical point-edge interaction network for point cloud semantic segmentation. In: Proceedings of IEEE Conference on Computer Vision & Pattern Recognition, 2019. 10433–10441
- 49 Choy C, Gwak J, Savarese S. 4D spatio-temporal ConvNets: Minkowski convolutional neural networks. In: Proceedings of IEEE Conference on Computer Vision & Pattern Recognition, 2019. 3075–3084
- 50 Qiu S, Anwar S, Barnes N. Semantic segmentation for real point cloud scenes via bilateral augmentation and adaptive fusion. In: Proceedings of the IEEE/CVF Conference on Computer Vision and Pattern Recognition (CVPR), 2021. 1757–1767
- 51 Hu Z, Zhen M, Bai X, et al. JSENet: joint semantic segmentation and edge detection network for 3D point clouds. In: Proceedings of European Conference on Computer Vision, 2020
- 52 Sauder J, Sievers B. Self-supervised deep learning on point clouds by reconstructing space. In: Proceedings of Conference on Neural Information Processing Systems, 2019. 12962–12972